Photochemistry and Photobiology, 2011, 87: 399–407

MPEG-hexPLA Micelles as Novel Carriers for Hypericin, a Fluorescent Marker for Use in Cancer Diagnostics

Karine Mondon, Magali Zeisser-Labouèbe, Robert Gurny and Michael Möller*

School of Pharmaceutical Sciences, Pharmaceutics, University of Geneva, University of Lausanne, Geneva, Switzerland

Received 8 June 2010, accepted 9 December 2010, DOI: 10.1111/j.1751-1097.2010.00879.x

ABSTRACT

Ovarian cancer is the most common gynecological cancer diagnosed in Western countries. Detection of micrometastases at an early stage of the disease could lead to a cure rate of 90% by limiting the spread of the disease outside the ovaries. In this article, hypericin (Hy), a hydrophobic photosensitizer used for the photodynamic diagnosis (PD) of ovarian cancer, was efficiently incorporated into a core of micelles made from methoxy-poly(ethylene glycol) and hexyl-substituted poly (lactides) copolymers. The fate of these micelles following intravenous injection was studied *in vivo* in two ovarian tumor-bearing animal models. In the chick embryo chorioallantoic membrane model, 17 times more Hy accumulated in tumor nodules when Hy was delivered with micelles than when Hy was delivered as an ethanol solution. Studies of the biodistribution of Hy in Fisher rats revealed escape of these nanosized micelles (< 32 nm) from the mononuclear phagocyte system. Hy-loaded micelles showed maximal accumulation in tumors and demonstrated the best tumor/muscle contrast visible 3 h after injection in the rat model. The rapid and highly selective accumulation of Hy in tumors that we demonstrated in this study suggests that these micelle formulations could be used for the PD of ovarian cancer in the future.

INTRODUCTION

In the current era, cancer is overtaking cardiovascular disease and becoming the leading cause of death worldwide. According to the World Health Organization, cancer-related deaths will reach 12 million in 2030 as compared to 7.4 million in 2004. Early detection of many types of cancers can reduce fatality rates by as much as 30%. Additionally, a precise localization of tumor tissues is essential before surgery, radiotherapy or chemotherapy is considered (1). Despite the progress that has been made in imaging technology (ultrasound, endoscopy and radiography), ovarian cancer is still the leading cause of death from gynecological malignancies in Western countries (2). Due to the absence of symptoms during the early stages of the disease, the majority of affected patients have already developed metastases when their cancer is diagnosed. As a consequence, the 5-year survival rate very much depends on the stage of the disease at the time of diagnosis. For stage I (localized) disease, the 5-year survival rate is 93%, whereas for stage IV (distant) disease, it decreases drastically to 31% (2). Early surgery combined with taxane- or platinum-based chemotherapy has improved the overall survival rate of ovarian cancer patients, but survival rates are still unacceptably low for patients with advanced disease. Half of these patients will relapse within 5 years after surgery (3), mainly due to nondetected residual metastases in the peritoneal cavity (4). A newly developed selective photodynamic diagnosis (PD) imaging technology has recently been shown to efficiently detect bladder cancer (5). This technique consists of administrating a photosensitizer (PS) or a precursor for the *in situ* formation of a PS, which preferentially accumulates in diseased tissues (6). Due to its fluorescence properties, the PS is easily located when excited at the appropriate wavelength, enabling easy detection of malignant tissues. Of the PS that has been studied, 5-aminolevulinic acid (5-ALA)-mediated protoporphyrin IX (PP IX), Photofrin®, Temoporfin (Foscan®) and Metvix® have been successfully used for the detection of various cancers (7), such as bladder (5), esophageal (8), skin (9) and head and neck cancer (10). In ovarian cancer, 5-ALA-mediated PP IX has shown feasibility and promise in detecting metastases in both animal models (11) and humans (4). Another PS that has been investigated for use in cancer detection is hypericin (Hy). Hy is an interesting PD compound due to its low photobleaching (12) and its natural origin as well as its photoactivity in several cancer cell lines (13–15) and rodent models (13,14,16). Recently, Hy has been found to be effective at detecting oral cancer (17) and bladder tumors in humans (18–21) as well as ovarian tumors in rats (22). Formulating Hy is a challenge due to its high degree of hydrophobicity (log P = 8.78 [23]). Polylactide (PLA) nanoparticles (Nps) loaded with Hy have recently been evaluated and have been shown to specifically reach tumor nodules in rats following intravenous (i.v.) administration. Because these polymeric Nps had a longer half-life as compared to the drug in solution as well as a small size (*ca* 200 nm), they were able to extravasate from the neovasculature and accumulate in diseased tissues through the enhanced permeation retention (EPR) effect (22,24). Their small size, long circulation time and specific accumulation and transport of the drug into tumor tissues are the reasons that there has been increasing interest in nanocarrier systems in cancer research (25–27).

Amongst the different nanocarrier systems that have been studied, polymeric micelles have gained special interest because

*Corresponding author email: michael.moeller@unige.ch (Michael Möller)

of their nanoscale small size, *in vivo* stability, high drug-loading capacity and good biocompatibility (28). Polymeric micelles have a specific core-shell structure formed by the self-assembly of amphiphilic copolymers. The outer shell, which is composed of a hydrophilic polymer, most often poly(ethylene glycol) (PEG), reduces interactions with blood proteins, facilitating a long circulation time. The inner core, which is formed by the hydrophobic block, can successfully be loaded with lipophilic drugs, such as PS (29–33). Biocompatible and biodegradable polymers like PLA are preferred for use in the hydrophobic core polymer, but some hydrophobic drugs can only be incorporated into PLA micelles in a limited fashion (34). Thus, it would be ideal to identify and create polymers with an increased degree of hydrophobicity that would allow more efficient drug loading, which, as a result, could lead to better clinical results.

Our group recently demonstrated the efficiency with which hydrophobic drugs, such as the PS meso-tetra(p-hydroxyphenyl)porphine (THPP) could be incorporated into hexyl-substituted poly(lactides) (hexPLA)-based micelles. These micelles were shown to load this hydrophobic drug more efficiently than standard PLA. Successful loading of 123 mg_{THPP} per $g_{copolymer}$ was achieved with methoxy-poly(ethylene glycol) (MPEG)–hexPLA, as compared to 62 mg_{THPP} per $g_{copolymer}$ that was achieved with MPEG–PLA micelles (35). To the best of our knowledge, there are no previous reports in the literature examining the potential pharmaceutical applications of polymeric micelle-incorporated Hy. In this paper, we investigated the potential utility of Hy formulated in MPEG–hexPLA micelle solutions in ovarian cancer diagnostics. Hy-loaded MPEG–hexPLA micelle formulations with a high drug-loading capacity were prepared and investigated in two different ovarian tumor-bearing animal models, the chick embryo chorioallantoic membrane (CAM) and the female Fisher rat F-344.

MATERIALS AND METHODS

Materials. Hypericin was purchased from Alexis Corporation (Lausen, Switzerland). Tetrahydrofuran (THF) was supplied by SDS (Toulouse, France). MPEG with a molecular weight of 2000 g mol^{-1} was a gift from Union Carbide Corporation (USA). D,L-lactide, tin(II) 2-ethylhexanoate ($Sn(Oct)_2$) and acetone p.a. were purchased from Purac Biochem (Gorinchem, The Netherlands), Aldrich (Buchs, Switzerland) and Fluka (Buchs, Switzerland), respectively, and used as received. The monomers mono-hexyl-substituted lactide and di-hexyl-substituted lactide were synthesized as described in a previous publication (36).

Synthesis and characterization of MPEG–hexPLA copolymers. The synthesis of MPEG–hexPLA copolymers with a molecular weight of approximately 5000 g mol^{-1} has been described previously (34,35). Briefly, MPEG–hexPLA copolymers were synthesized by ring opening polymerization with a MPEG of 2000 g mol^{-1} as the initiator and tin octanoate as the catalyst. The obtained copolymers were characterized by their molecular weight (M_n) and polydispersity index (P.I.) by gel permeation chromatography. The structures of MPEG–hexPLA are presented in Scheme 1.

Preparation of Hy-loaded MPEG–hexPLA micelles. Hy-loaded MPEG–hexPLA micelles were prepared by the cosolvent evaporation method described by Mondon *et al.* (37). Briefly, 100 mg mL^{-1} solutions of MPEG–hexPLA copolymers in acetone and a 10 mg mL^{-1} solution of Hy in acetone were prepared. Next, 500 μL or 200 μL of Hy solution were gently mixed with 400 μL of MPEG–dihexPLA or 800 μL of MPEG–monohexPLA solution, respectively. Acetone was added to the organic phase in order to obtain a final volume of 1 mL. The organic mixture was poured into 2 mL isotonic saline solution under sonication and then slowly removed by evaporation at 15 mbar. The final micelle concentrations were adjusted by adding isotonic saline solution to reach a copolymer concentration of 20 mg mL^{-1} for MPEG–dihexPLA and 40 mg mL^{-1} for MPEG–monohexPLA (see structural difference in Scheme 1). The solutions were left to equilibrate overnight and then centrifuged at 9500 ***g*** for 15 min to remove nonincorporated Hy. Both MPEG–hexPLA micelles were then analyzed for size and drug loading.

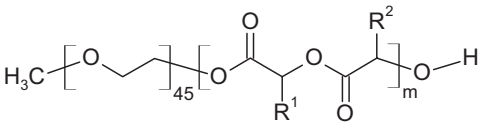

$R^1=C_6H_{13}$, $R^2=CH_3$: $MPEG_{2000g/mol}$-$monohexPLA_{3000g/mol}$ for m=14
R^1, $R^2=C_6H_{13}$: $MPEG_{2000g/mol}$-$dihexPLA_{3000g/mol}$ for m=11

Scheme 1. Structure of MPEG–hexPLA block copolymers.

Characterization of Hy-loaded MPEG–hexPLA micelles. The hydrodynamic (Z_{av}) and number-weighted (d_n) diameters of micelles were measured by dynamic light scattering after centrifugation. Analyses were performed at 25°C with a Zetasizer HS 3000 system (Malvern, Worcestershire, UK) at an angle of 90°. For each sample, mean diameters were obtained after 3 runs of 10 measurements.

For drug-loading determination, the micelles were broken up by a 10-fold dilution with acetone. The released Hy was quantified in triplicate by reversed-phase HPLC as previously described by Zeisser-Labouèbe *et al.* (38). The HPLC was calibrated with standard solutions of 2.0–200 μg mL^{-1} of Hy dissolved in acetone. The resulting calibration curves were obtained with regression coefficients greater than 0.99.

The incorporation efficiency and drug loading were calculated using Eqs. (1) and (2), respectively:

$$\text{Incorporation efficiency } (\%) = \frac{\text{mass of drug incorporated in micelles (g)}}{\text{mass of drug introduced (g)}} \times 100 \quad (1)$$

$$\text{Drug loading } (\%\text{wt/wt}) = \frac{\text{mass of drug incorporated in micelles (g)}}{\text{mass of copolymer used (g)}} \times 100 \quad (2)$$

Animals. Female Fisher rats F-344 (150–200 g) were purchased from Charles River Laboratories (L'Arbresle, France) and housed in a temperature-controlled room with a 12 h light/dark cycle. They were given a commercial basal diet and water *ad libitum*. All animal experiments and animal husbandry were carried out in compliance with national regulations and approved by the cantonal veterinary office of Geneva, Switzerland (Certificate number 31.1.1020/3065/2).

Cell culture and cell preparation for in vivo inoculation. The NuTu-19 cell line, a poorly differentiated Fisher 344 rat-derivative epithelial ovarian cancer cell line (39), was kindly provided by Dr. A. Major (Geneva University Hospital, Geneva, Switzerland). The cells were cultured in Dulbecco's Modified Eagle's medium (Gibco Life Technologies, Carlsbad) supplemented with 10% fetal bovine serum (Brunschwig, Amsterdam, The Netherlands) and 100 U mL^{-1} penicillin–streptomycin (Gibco Life Technologies) at 37°C (atm. 5% CO_2). Before tumor implantation onto the CAM or into rats, NuTu-19 cells were washed twice with phosphate buffered saline (Gibco Life Technologies, Carlsbad), harvested using 0.5% Trypsin–EDTA (Gibco Life Technologies, Carlsbad) and counted. After centrifugation, an equal mixture of complete culture medium and Matrigel™ matrix (BDBiosciences, Bedford) was prepared. A suspension of 10^8 cells mL^{-1} was prepared for the CAM experiments and a suspension of 5×10^6 cells mL^{-1} was prepared for the rat experiments.

Chick embryo CAM study. The chick embryo CAM model was adapted from the model described by Lange *et al.* (40). Egg incubation was performed according to the procedure described by Vargas *et al.* (24,41). Briefly, fertilized hen eggs, which were kindly provided by the Geneva University Animal House (Geneva, Switzerland) were placed with the narrow apex down in an incubator (Savimat MG 200, Chauffry, France) at 37°C with a relative humidity of 65%. The eggs

were rotated twice a day until embryo development day 3 (EDD3). On EDD4, a 3 mm hole was drilled into the eggshell and the narrow apex was covered with an adhesive tape. The eggs were incubated in a static mode until EDD8, when the hole in the eggshell was enlarged by 2 or 3 mm to allow the placement of a silicon O-ring (Apple Rubber Products, Inc., Lancaster) on the CAM. Next, 20 μL of the ovarian cancer NuTu-19 cell suspension (10^8 cells mL^{-1}) were inoculated topically to allow tumor growth inside the O-ring area. The open hole was then sealed with a plastic film (Parafilm; Pechiney Plastic Packaging, Chicago) to avoid contamination and desiccation of the CAM. Eggs were returned to the static incubator until EDD12, the day of the test formulation administration. A total of three formulations were tested on five eggs each: (1) an Hy-loaded MPEG–monohexPLA formulation with a concentration of 0.69 mg mL^{-1} Hy; (2) an Hy-loaded MPEG–dihexPLA formulation with a concentration of 1.0 mg mL^{-1} Hy; and (3) a Hy solution (1.0 mg mL^{-1} Hy in a mixture of ethanol, PEG 400 and water). These formulations were injected *via* the main vessel of the CAM at a dose of 2 mg kg^{-1} (*i.e.* 20 ng per egg). The eggs were returned to the incubator and the fluorescence of the tumor nodules was evaluated at 1 min, 1 h, 3 h and 6 h postinjection by fluorescence microscopy with an attenuation coefficient of 4 (see details of the set-up in reference [24]).

The relative tumor fluorescence (F_{rel}) was calculated using Eq. (3):

$$F_{rel} = \frac{(F_t - F_0)}{F_0}, \quad (3)$$

where F_t is the tumor fluorescence intensity at the different time points and F_0 is the tumor autofluorescence prior to drug injection.

Biodistribution of Hy-loaded MPEG–dihexPLA micelles in rats. Ovarian tumor-bearing female Fisher rats (F-344) were used for Hy biodistribution studies. The rats were inoculated intraperitoneally with 1 mL of ovarian cancer NuTu-19 cell suspension (5×10^6 cells) to induce tumor growth. After 5 weeks, ascites were palpable and tumors had grown sufficiently to allow us to perform the study. The rats were injected intravenously in the tail vein with Hy formulations at a dose of 2 mg kg^{-1}. Three formulations were investigated: (1) Hy-loaded MPEG–dihexPLA micelles; (2) Hy solution (2 mg mL^{-1} in a mixture of ethanol, PEG 400 and water); and (3) isotonic saline solution (which was administered to two rats as a control). After intravenous injection of the Hy formulations, four rats per formulation were sacrificed by CO_2 asphyxia at 1, 3, 6 and 24 h after injection for the micelle formulations and 1 h after injection for Hy in ethanol solution. In order to visualize the tumors by fluorescence imaging, the abdominal cavity was opened and images were compared under white and blue light, respectively using the set-up described previously by Zeisser-Labouèbe *et al.* (22). Blood samples were obtained by cardiac puncture with heparinized tubes. The liver, spleen, lung, tumor and muscles surrounding the tumors were excised. All samples were weighed and stored at −20°C until analysis. Tissue samples were extracted with THF complemented with a tissue homogenizer (Eurostar digital, IKA®-Werke, Staufen, Germany). Blood samples were prepared for analysis by THF extraction and sonication (five times for 5 s with a sonifier S-450D®, Branson Ultrasonic S.A, Geneva, Switzerland). After sample centrifugation, the supernatants were evaporated under nitrogen. The residues were dissolved in 0.3 mL DMSO and their Hy fluorescence was determined with a microplate reader (Safire®, Tecan, Salzburg, Austria) at the excitation and emission wavelengths of 530 and 645 nm. The obtained fluorescence intensity was corrected by subtraction of the fluorescence of control samples. The respective Hy concentration was calculated from the calibration curve (1.95–25 ng mL^{-1}), which had a regression coefficient higher than 0.999.

Stability of Hy-loaded MPEG–dihexPLA micelles in blood plasma. Human blood plasma from an anonymous AB donor (Geneva University Hospital, Switzerland) was used for the study of the stability of Hy-loaded MPEG–dihexPLA micelles in the presence of plasma. A volume of 187 μL Hy-loaded MPEG–dihexPLA micelles was added and mixed with 12 mL plasma for 1, 3, 6 and 24 h in the dark at 37°C under orbital shaking to mimic the experimental conditions of the *in vivo* studies. A control experiment with Hy solution (2 mg mL^{-1} in a mixture of ethanol, PEG 400 and water) was also carried out under the same conditions, except that 94 μL of the Hy solution were mixed with 6 mL plasma. After shaking, 4 mL of the plasma/micelles mixture were centrifuged for 5 min at 8500 ***g*** (Beckman, Avanti™, Fullerton) in order to remove nonentrapped drug. One milliliter of the supernatant was dissolved in 2 mL THF under sonication. The resulting organic mixture was afterward centrifuged for 5 min at 8500 ***g*** to remove blood components that have precipitated with the addition of THF. The entire remaining supernatant was collected, dried and dissolved in 400 μL acetone. The acetone solution was finally centrifuged to remove all other precipitates (5 min, 8500 ***g***), and directly analyzed (with no dilution) by HPLC for the Hy drug content.

Please note that the used volume of blood plasma was chosen to simulate the *in vivo* concentrations in the animal model, and was calculated from the following Eq. (4) for the blood volume and the body weight of the rats (42):

$$\text{Blood volume (mL)} = 0.06 \times \text{body weight (g)} + 0.77 \quad (4)$$

Here, the body weight corresponded to 187 g, the average body weight calculated from the 22 rats studied in the *in vivo* experiments.

Statistical analysis. Results are expressed as means ± SD (standard deviations). The significance of between-group differences was determined using Student's *t*-test. All *P*-values < 0.05 were considered to be statistically significant.

RESULTS

Hypericin/MPEG–hexPLA micelle formulations

Hypericin-loaded micelle formulations were prepared for *in vivo* evaluation in the CAM model. Table 1 shows the size characteristics and Hy incorporation of these micelles. MPEG–monohexPLA and MPEG–dihexPLA micelles had d_n of 32 nm and of 19 nm and mean Z_{av} of 133 nm and 85 nm, respectively. The high Hy incorporation efficiency that we observed ($> 70\%$) yielded a Hy solubility of 0.69 mg mL^{-1} for MPEG–monohexPLA micelles and 2.02 mg mL^{-1} for MPEG–dihexPLA micelles. These values correspond to a drug-loading of 1.7% and 9.8% (%wt/wt), respectively. It is notable that with the MPEG–dihexPLA micelles, half of the amount of excipient was needed to create a formulation with double the Hy concentration in comparison to the less hydrophobic MPEG–monohexPLA.

Chick embryo CAM study

Four days after topical inoculation of NuTu-19 cells onto the CAM (which occurred on EDD8), visible tumor nodules with

Table 1. Hy-loaded MPEG–monohexPLA and MPEG–dihexPLA micelle formulations and characteristics.

Polymeric micelles	M_n (g mol^{-1})	M_n/M_w	Copolymer concentration	Hy concentration	Incorporation efficiency	Drug loading (%wt/wt)	Z_{av} (nm)	P.I.	d_n	[%]d_n
MPEG–monohexPLA	5600	1.15	40 mg mL^{-1}	0.69 mg mL^{-1}	69.6%	1.7	133	0.1	32	100
MPEG–dihexPLA	5351	1.12	20 mg mL^{-1}	2.02 mg mL^{-1}	80.8%	10.2	85	0.3	19	100

Hy = hypericin; MPEG = methoxy-poly(ethylene glycol); monohexPLA = mono-hexyl-substituted polylactide; dihexPLA = di-hexyl-substituted polylactide; M_n/M_w = molecular weight; Z_{av} = hydrodynamic diameter; P.I. = polydispersity index; d_n = number-weighted diameter.

extensive neovascularization were observed at the membrane surface. Hy-loaded micelles and the Hy solution were injected at the same dose (2 mg kg^{-1}). The fluorescence intensity of the accumulated Hy in the nodules was observed and photographed 1 min, 1 h, 3 h and 6 h following the administration. The corresponding fluorescence images showed the increase in fluorescence intensity over time within the ovarian tumor nodules as compared to the nontumoral surrounding tissues (Fig. 1). Compared to Hy in solution (upper row), both Hy-loaded MPEG–hexPLA micelle formulations (lower row) led to a much higher fluorescent signal in the nodules. The higher accumulation of Hy within the tumors was confirmed by the plot of the F_{rel} intensity *versus* time (Fig. 2). No statistically significant differences were found between the two micelle formulations. However, the micelle formulations led to a significantly higher fluorescence as compared to the drug in solution at all time points ($P < 0.05$). Six hours after injection, the fluorescence intensity in the tumor nodules that was achieved by the MPEG–hexPLA micelle formulations was 13–17 times higher than that achieved by the Hy in ethanol solution.

Biodistribution of Hy-loaded MPEG–dihexPLA micelles

The biodistribution of Hy-loaded micelles was investigated following injection into Fisher rats at a dose of 2 mg kg^{-1} body weight. In this experiment, the Hy-MPEG–dihexPLA formulation with the higher drug-loading efficiency (at a concentration of 1 mg mL^{-1}) was chosen. Hy in a clear ethanol–PEG 400-water solution was used for comparison. No sign of precipitation was visually observed at the site of injection for both tested solutions. The plasma Hy concentration profiles observed for the Hy solution and Hy-loaded micelles are shown in Fig. 3. The results for the Hy solution concerning the 3, 6 and 24 h time points were taken from the published work of Zeisser-Labouèbe *et al.* (who performed their studies on Fisher 344 rats) (22). At all tested time points, the Hy plasma levels that were obtained were significantly higher when Hy was incorporated into micelles as compared to Hy in ethanol solution. At 1 h after injection, Hy loaded in micelles showed a plasma concentration that was six times higher concentration than was achieved when the rats were injected with ethanol solution. After 3 h, the plasma concentration achieved by the Hy-loaded micelles was four times higher than was achieved with Hy in ethanol solution and after 6 h, it was two times higher. After 24 h, the plasma concentration achieved by the Hy-loaded micelles was three times higher than for the drug in solution, indicating that the circulation time of Hy was significantly prolonged when it was incorporated in the micelle carriers.

The distribution of both micelle formulations that were tested in rat livers, spleens and lungs is illustrated in Fig. 4. The uptake of Hy following administration of Hy in solution was higher in the spleen than in the lungs and liver. Hy delivered in micelles was found in higher concentrations in the spleen and lungs than in the liver. A total of 24 h after

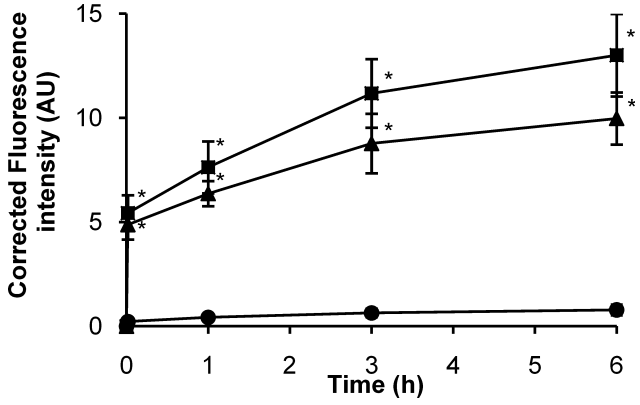

Figure 2. Relative tumor fluorescence intensity over time after i.v. administration of hypericin (Hy)-loaded MPEG–monohexPLA micelles (■), MPEG–dihexPLA micelles (▲) and Hy solution (●) at a dose of 2 mg kg^{-1} in chick embryos (mean ± SD, $n = 5$). *Significantly different from chick embryos injected with Hy solution (Student's *t*-test, $P < 0.05$). MPEG = methoxy-poly(ethylene glycol); monohexPLA = mono-hexyl-substituted polylactide.

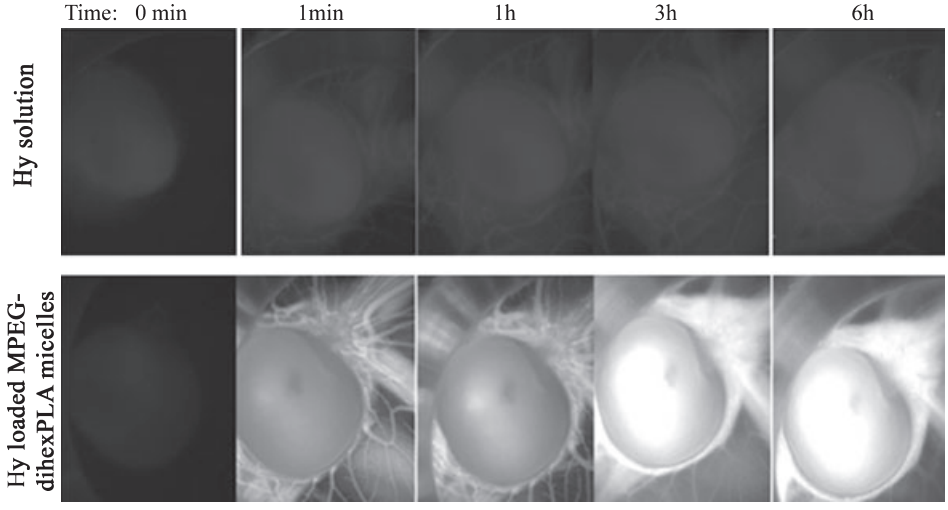

Figure 1. Fluorescence images of nodules after injection of hypericin (Hy) in solution and Hy-loaded MPEG–dihexPLA micelle formulation at a dose of 2 mg kg^{-1} in chick embryo (chorioallantoic membrane model). MPEG = methoxy-poly(ethylene glycol); dihexPLA = di-hexyl-substituted polylactide.

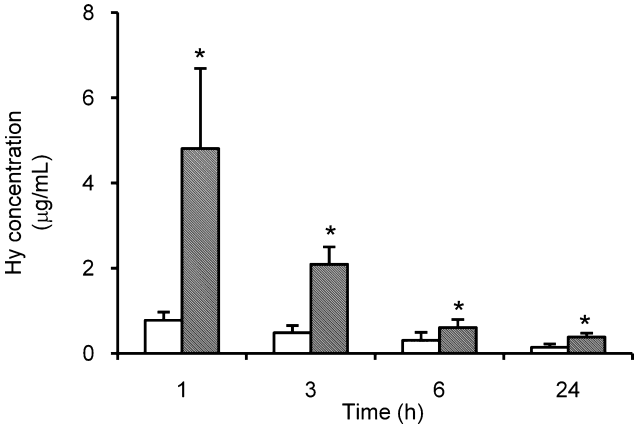

Figure 3. Plasma concentration profile of hypericin (Hy) after i.v. injection in rats of Hy solution (white bars) and of Hy-loaded MPEG–dihexPLA micelles (dashed bars) at a dose of 2 mg kg^{-1}. (mean ± SD, n = 3–4). *Significantly different from rats injected with Hy solution (Student's t-test, $P < 0.05$). Results of Hy in solution after 3, 6 and 24 h were taken from reference (22). MPEG = methoxy-poly(ethylene glycol); dihexPLA = di-hexyl-substituted polylactide.

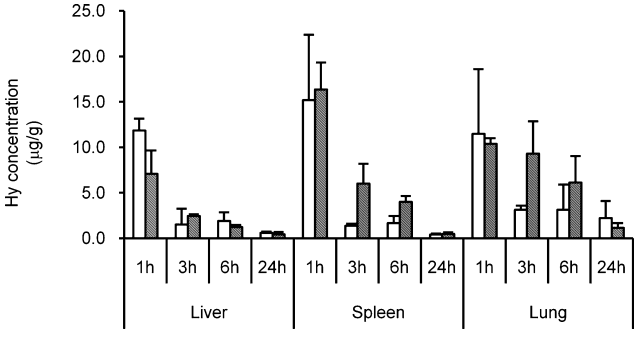

Figure 4. Biodistribution of hypericin (Hy) in liver, spleen and lung over time after injection of Hy solution (white bars) and of Hy-loaded MPEG–dihexPLA micelles (dashed bars) at a dose of 2 mg kg^{-1} in rats (mean ± SD, n = 3–4). Results of Hy in solution after 3, 6 and 24 h were taken from reference (22). MPEG = methoxy-poly(ethylene glycol); dihexPLA = di-hexyl-substituted polylactide.

administration, Hy that had been loaded in micelles was eliminated by these organs at the same rate as the drug solution. Both formulation profiles were similar for the liver and led to a final Hy concentration of 0.60 and 0.43 μg g^{-1} tissue when Hy was delivered in solution and in micelles, respectively. Hy-loaded micelles exhibited a slower elimination from the spleen than Hy in ethanol solution at 1 h, 3 h and 6 h after injection, but showed the same concentration after 24 h. In the lungs, Hy loaded in micelles showed a similar profile as in the spleen, except that after 24 h, Hy that had been administrated in micelle formulations was more rapidly eliminated than the drug solution.

In addition to examining the tissue distribution of Hy, we also determined the accumulation of Hy-loaded MPEG–dihexPLA micelle in the tumors and surrounding muscle tissue. For both tested formulations, the Hy concentration in the surrounding muscles was very low as compared to the

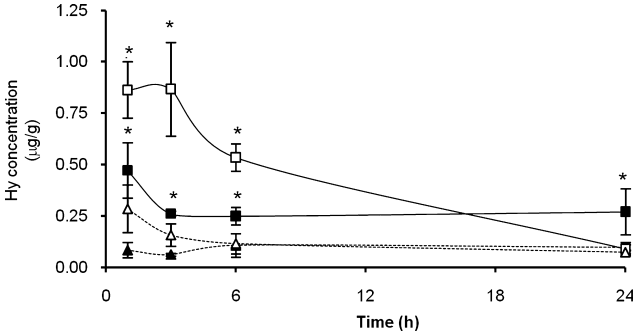

Figure 5. Biodistribution of hypericin (Hy) in tumors (open symbols) and the surrounding muscle (plain symbols) over time after injection of Hy solution (△, ▲) and of Hy-loaded MPEG–dihexPLA micelles (□, ■) at a dose of 2 mg kg^{-1} in rats (mean ± SD, n = 3–4). *Significantly different from rats injected with Hy solution (Student's t-test, $P < 0.05$). Results of Hy in solution after 3, 6 and 24 h were taken from reference (22). MPEG = methoxy-poly(ethylene glycol); dihexPLA = di-hexyl-substituted polylactide.

concentration that was observed in the other investigated organs. However, a slightly higher Hy accumulation in muscles was observed for Hy-loaded micelles as compared to Hy in solution. In the tumors, a significant accumulation of Hy-loaded micelles was found for the first 6 h after injection, with a maximum level detected at 3 h (Fig. 5). After 24 h, the Hy accumulation decreased to a concentration that was similar to the concentration that was obtained with the drug in solution.

For the application of Hy-loaded micelles to be successful for tumor imaging, a high contrast between healthy tissues (muscle) and diseased tissues (tumor) is essential. The visual distinction between these tissues is possible by using endoscopy with blue light. Under white light, no difference between muscle tissues and tumor nodules could be observed (Fig. 6). However, under blue light, the red fluorescence of Hy accumulated in the tumor nodules became clearly visible, while the absence or near absence of red fluorescence in the healthy muscle indicated the absence or very low accumulation of Hy. Visually, the maximum contrast between healthy and diseased tissues was observed 3 h after micelle injection. To achieve more quantitative measurements, the tumor-to-muscle ratio was calculated from the extracted and analyzed Hy concentrations. This analysis also found that the highest contrast between tumor and muscle tissue was present 3 h after injection of Hy-loaded micelles (Fig. 7). It is also worth noting that this time was also the point at which maximum concentration of the fluorescent marker could be detected in the tumor tissue (Fig. 5).

Stability of Hy-loaded MPEG–dihexPLA micelles in blood plasma

The stability of Hy-loaded micelles has been studied in blood plasma and has been performed under similar conditions as in the *in vivo* experiments, *i.e.* with the same dilution factor and the same dose. Hy-loaded micelles retained more than 80% of the introduced Hy quantity in plasma at all the tested time points (1, 3, 6 and 24 h), whereas for the control of Hy in ethanol solution only 10–15% of Hy was found in the plasma (Fig. 8).

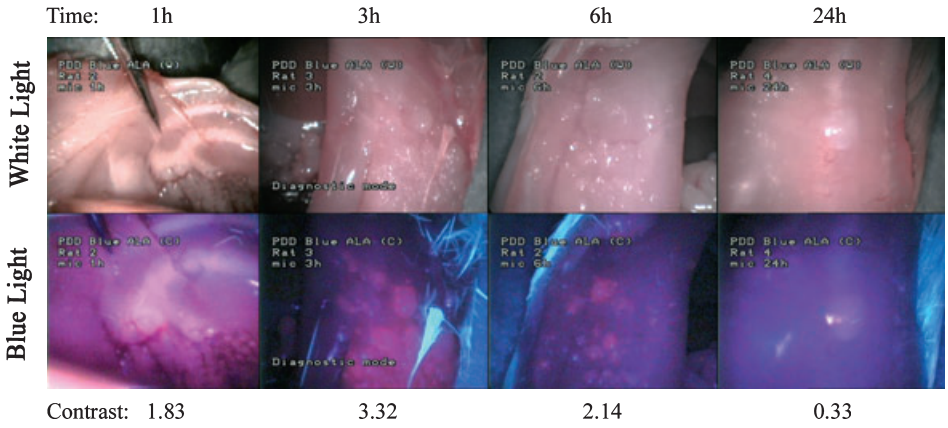

Figure 6. Pictures of ovarian metastasis in the peritoneal cavity of rats under (a) white light and (b) blue light after injection of hypericin (Hy)-loaded MPEG–dihexPLA micelles. Below, the given contrast was obtained between diseased tissues and surrounding healthy muscle. MPEG = methoxy-poly(ethylene glycol); dihexPLA = di-hexyl-substituted polylactide.

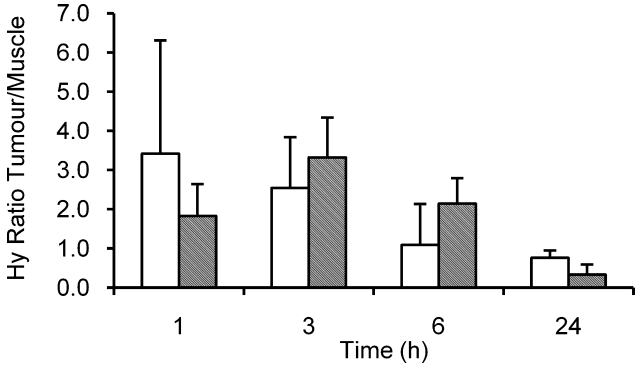

Figure 7. Tumor-to-muscle contrast over time after injection of hypericin (Hy) solution (white bars) and of Hy-loaded MPEG–dihexPLA micelles (dashed bars) at a dose of 2 mg kg^{-1} in rats. Results of Hy in solution after 3, 6 and 24 h were taken from reference (22). MPEG = methoxy-poly(ethylene glycol); dihexPLA = di-hexyl-substituted polylactide.

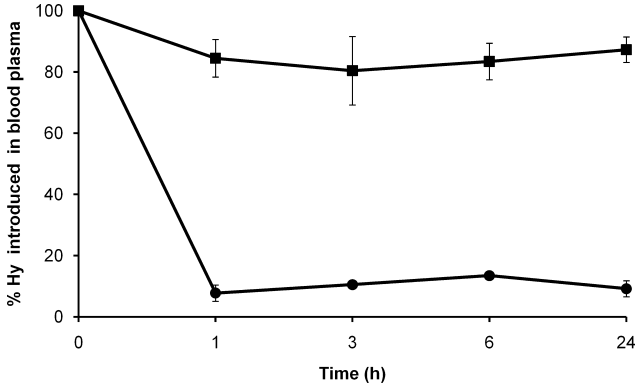

Figure 8. Percentage of hypericin recuperated from human blood plasma when added as an ethanol solution (●) and when added within MPEG–dihexPLA micelles (■), respectively. MPEG = methoxy-poly(ethylene glycol); dihexPLA = di-hexyl-substituted polylactide.

DISCUSSION

Over the last decades, nanosized polymeric micelles have become a topic of increasing interest in the field of drug delivery. Because of their specific core-shell structure, they can carry potent hydrophobic drugs within their core, while their hydrophilic shell facilitates water solubility. Their ability to accumulate at tumor sites *via* the EPR effect envisions localized cancer treatments (43).

In the present study, the objective was to investigate novel MPEG–hexPLA micelles for their potential use in ovarian cancer diagnosis. We examined their ability to achieve efficient drug loading, a long circulation time and selective accumulation in tumor tissue in a series of *in vivo* experiments. As demonstrated, the relatively water insoluble fluorescent marker Hy was successfully incorporated into MPEG–hexPLA micelles, reaching an aqueous solubility of *ca* 2 mg mL^{-1}, which represents a high increase in its water solubility as compared to the drug alone. In addition, incorporating Hy in MPEG–hexPLA micelles increased its circulation time in the bloodstream, which is a major advantage for passive tumor targeting. Even 24 h after injection into ovarian tumor-bearing rats, Hy-loaded MPEG–dihexPLA micelles were still present in the plasma. The distribution of Hy has been proven *in vitro* to be due to Hy stably incorporated into micelles for 24 h and not gradually released from the micelles. The loss of Hy when added within micelles in human blood plasma ($<20\%$) observed after 1 h can be explained either by the multiple steps needed for the extraction of the drug, by a possible equilibrium needed to be reached during the first hour between the micelles and the plasma components, or by both phenomena. The observed low Hy plasma concentration even after 1 h can be attributed to a probably very fast decrease of the Hy-loaded micelle concentration in the blood between the injection and the first studying time point. Indeed, a study with comparable MPEG–PLA micelles (molecular weight around 5000 g mol^{-1} with MPEG 2000 g mol^{-1}) and with paclitaxel as the incorporated drug demonstrated a biphasic nature of the plasma profile with an initial fast distribution phase completed within the first hour (44). The presence of inert hydrophilic PEG on the nanocarrier surface provided good steric hindrance, limiting blood serum protein binding and as expected increasing the carrier's circulation time (45,46). In addition, the increased hydrophobicity of the hexPLA core, in comparison to a PLA or PCL micelle core,

allowed the novel MPEG–dihexPLA micelles to have a lower critical micelle concentration (47), thus a higher stability upon dilution, and a higher stability in PBS modeling intravenous conditions (pH 7.4 at 37°C) (48), consequently increasing the life time of the Hy loaded in micelles in the blood stream.

For cancer diagnosis, increased accumulation of the fluorescent marker at the tumor sites enables better tumor detection. In both *in vivo* studies, Hy-loaded micelles primarily accumulated in ovarian tumors, thereby meeting this requirement. The accumulation of free Hy is often associated with aggregation, and a possible loss of fluorescence intensity. Here, this quenching phenomenon is not likely to occur as Hy released from the micelles at the site of interest would not aggregate due to the presence of proteins like LDL, HDL or albumin (49,50) to which Hy rapidly binds and does not influence the fluorescence properties. In the CAM studies, accumulated Hy-loaded micelles showed a much higher intensity of fluorescence as reported for Hy-loaded Nps (24). A five-fold increased accumulation of Hy in tumors was obtained with Hy-loaded MPEG–hexPLA micelles as compared to Hy-loaded Nps 3 h after injection. In ovarian tumor-bearing rats, the biodistribution study confirmed that Hy micelles rapidly accumulated in tumor tissues at high concentrations. Hy loaded in MPEG–dihexPLA micelles reached a maximum concentration and a maximum tumor-to-muscle contrast 3 h after injection. In contrast Hy-Nps showed its highest accumulation 24 h after injection (22). The differences that were observed in the tumor accumulation profiles between the two animal models (rat *versus* CAM) can be attributed to the absence of an elimination process in the CAM model (24). In the rat experiments, the differences between the two Hy nanocarriers (*i.e.* micelles and Nps) can be explained by differences in the size of the two carrier systems. It has been reported that the accumulation effect is primarily influenced by the size of the carrier (51). Because of their small size, nanocarriers can easily pass through the gaps in leaky endothelial walls and are efficiently taken up by tumor cells. Nagayasu *et al.* reported that for liposomes, a diameter of ≤100 nm seemed to be most suitable in order to achieve a long half-life in the blood circulation, tumor-specific drug accumulation and *in vivo* drug release (52). Moreover, another biological process of micelle uptake in tumor tissues has recently been described by Kawaguchi *et al.* (53). They discovered by histological tracking that labeled PEG-poly(aspartate) copolymer micelles accumulated more rapidly (after 1 h) *via* the blood vessels at the tumor periphery than *via* tumor blood vessels due to the EPR effect. The Hy-loaded MPEG–hexPLA micelles (Z_{av} = 90 nm and $d_n <$ 30 nm) accumulated faster and more efficiently in tumors 3 h after injection than Hy–PLA Nps (Z_{av} = 200–300 nm), which needed at least 24 h to reach their highest accumulation (22). For the MPEG–hexPLA formulations, it was found that the disappearance of Hy from the bloodstream coincided with Hy uptake in tissues and, more specifically, tumor uptake. The decrease in plasma Hy concentration 6 h after injection demonstrates the elimination of Hy and Hy-loaded MPEG–hexPLA micelles from the bloodstream. Similarly, Burt *et al.* showed that MPEG–PLA copolymers were rapidly eliminated from the body through the urine (44). The degradation of the copolymer in acidic conditions, which are present in tumor tissues, is one plausible explanation (54,55). The emerging lower molecular weight components are also more rapidly filtered and eliminated by the kidneys (29,56). This suggests a low risk of chronic accumulation of a micelle formulation in the human body if it were to be administered in a clinical setting.

With regard to the need for an early detection of ovarian cancer and any metastases that are present that was discussed above, it can be concluded that Hy-loaded MPEG–hexPLA formulations lead to a rapid (3 h) accumulation of the fluorescent marker in rat tumors with an excellent contrast to surrounding healthy tissues. When one considers the procedures that are currently practiced in the clinical setting, it becomes apparent that laparoscopic examination using blue light following intravenous administration of Hy micelle formulations could increase the visualization of tumors and micrometastases in the pelvis. This would allow for a efficient, early diagnosis of ovarian cancer. It would also lead to more accurate staging. Both of these factors could result in improved patient prognosis due to earlier identification of the appropriate treatment regimen for each patient. Follow-up laparoscopic examinations should be possible with the same efficacy, since the very small size MPEG–hexPLA micelles should not induce the accelerated blood clearance phenomenon that is often observed with pegylated nanoassemblies > 50 nm following a second injection (57,58). In addition to cancer diagnosis, laparoscopy under blue light could be performed during surgery, facilitating complete removal of diseased tissues. For both of these possible clinical applications, the fast and efficient micelle accumulation that can be achieved with these formulations is a great advantage, since it can reduce the time needed for a routine patient check-up or preparation prior to a necessary surgery. The proof of concept that we achieved in the CAM and rat model showed promising results. In view of their possible clinical applications, MPEG/dihexPLA molecular weights and ratios could be further tailored to modulate and optimize their circulation time, loading capacity and diagnostic properties in future studies.

Acknowledgement—The authors would like to thank the Swiss National Science Foundation (SNF) for its financial support (SNF 200020-103752).

REFERENCES

1. Hennessy, B. T., R. L. Coleman and M. Markman (2009) Ovarian cancer. *Lancet* **374**, 1371–1382.
2. Jemal, A., R. Siegel, E. Ward, Y. Hao and M. J. Thun (2009) Cancer statistics, 2009. *CA Cancer J. Clin.* **59**, 225–249.
3. Collinet, P., F. Sabban, M. O. Farine, R. Villet, D. Vinatier and S. Mordon (2007) Laparoscopic photodynamic diagnosis of ovarian cancer peritoneal micro metastasis: An experimental study. *Photochem. Photobiol.* **83**, 647–651.
4. Löning, M., H. Diddens, K. Diedrich and G. Hüttmann (2004) Laparoscopic fluorescence detection of ovarian carcinoma metastases using 5-aminolevulinic acid-induced protoporphyrin IX. *Cancer* **100**, 1650–1656.
5. Song, X., Z. Ye, S. Zhou, W. Yang, X. Zhang, J. Liu and Y. Ma (2007) The application of 5-aminolevulinic acid-induced fluorescence for cystoscopic diagnosis and treatment of bladder carcinoma. *Photodiagnosis Photodyn. Ther.* **4**, 39–43.
6. Hillemanns, P., P. Soergel and M. Löning (2009) Fluorescence diagnosis and photodynamic therapy for lower genital tract diseases—A review. *Med. Laser Appl.* **24**, 10–17.

7. Allison, R. R. and C. H. Sibata (2010) Oncologic photodynamic therapy photosensitizers: A clinical review. *Photodiagnosis Photodyn. Ther.* **7**, 61–75.
8. Moghissi, K., K. Dixon, M. Stringer and J. A. C. Thorpe (2009) Photofrin PDT for early stage oesophageal cancer: Long term results in 40 patients and literature review. *Photodiagnosis Photodyn. Ther.* **6**, 159–166.
9. Lopez, R. F. V., N. Lange, R. Guy and M. V. Lopes Badra Bentley (2004) Photodynamic therapy of skin cancer: Controlled drug delivery of 5-ALA and its esters. *Adv. Drug Deliv. Rev.* **56**, 77–94.
10. Lorenz, K. J. and H. Maier (2008) Squamous cell carcinoma of the head and neck. Photodynamic therapy with Foscan®. *HNO* **56**, 402–409.
11. Ascencio, M., M. Delemer, M. O. Farine, E. Jouve, P. Collinet and S. Mordon (2007) Evaluation of ALA-PDT of ovarian cancer in the Fisher 344 rat tumor model. *Photodiagnosis Photodyn. Ther.* **4**, 254–260.
12. Pytel, A. and N. Schmeller (2002) New aspect of photodynamic diagnosis of bladder tumors: Fluorescence cytology. *Urology* **59**, 216–219.
13. Saw, C. L. L., M. Olivo, K. C. Soo and P. W. S. Heng (2006) Delivery of hypericin for photodynamic applications. *Cancer Lett.* **241**, 23–30.
14. Liu, C. D., D. Kwan, R. E. Saxton and D. W. McFadden (2000) Hypericin and photodynamic therapy decreases human pancreatic cancer in vitro and in vivo. *J. Surg. Res.* **93**, 137–143.
15. Colasanti, A., A. Kisslinger, R. Liuzzi, M. Quarto, P. Riccio, G. Roberti, D. Tramontano and F. Villani (2000) Hypericin photosensitization of tumor and metastatic cell lines of human prostate. *J. Photochem. Photobiol. B* **54**, 103–107.
16. Uzdensky, A., V. Iani, L. W. Ma and J. Moan (2006) On hypericin application in fluorescence diagnosis and cancer treatment: Pharmacokinetics and photosensitizing efficiency in nude mice bearing WiDr carcinoma. *Med. Laser Appl.* **21**, 271–276.
17. Thong, P. S. P., M. Olivo, W. W. L. Chin, R. Bhuvaneswari, K. Mancer and K. C. Soo (2009) Clinical application of fluorescence endoscopic imaging using hypericin for the diagnosis of human oral cavity lesions. *Br. J. Cancer* **101**, 1580–1584.
18. Kubin, A., P. Meissner, F. Wierrani, U. Burner, A. Bodenteich, A. Pytel and N. Schmeller (2008) Fluorescence diagnosis of bladder cancer with new water soluble hypericin bound to polyvinylpyrrolidone: PVP-hypericin. *Photochem. Photobiol.* **84**, 1560–1563.
19. Sim, H. G., W. K. Lau, M. Olivio, P. H. Tan and C. W. Cheng (2010) Is photodynamic diagnosis using hypericin better than white-light cystoscopy for detecting superficial bladder carcinoma? *BJU Int.* **95**, 1215–1218.
20. D'Hallewin, M. A., L. Bezdetnaya and F. Guillemin (2002) Fluorescence detection of bladder cancer: A review. *Eur. Urol.* **42**, 417–425.
21. D'Hallewin, M. A., P. A. De Witte, E. Waelkens, W. Merlevede and L. Baert (2000) Fluorescence detection of flat bladder carcinoma in situ after intravesical instillation of hypericin. *J. Urol.* **164**, 349–351.
22. Zeisser-Labouèbe, M., F. Delie, R. Gurny and N. Lange (2009) Benefits of nanoencapsulation for the hypericin-mediated photodetection of ovarian micrometastases. *Eur. J. Pharm. Biopharm.* **71**, 207–213.
23. United States National Library of Medicine (2010) Available after search of "Hypericin" at: http://chem.sis.nlm.nih.gov/chemidplus/
24. Zeisser-Labouèbe, M., F. Delie, R. Gurny and N. Lange (2009) Screening of nanoparticulate delivery systems for the photodetection of cancer in a simple and cost-effective model. *Nanomedicine* **4**, 135–143.
25. Singh, R. and J. Lillard (2009) Nanoparticle-based targeted drug delivery. *Exp. Mol. Pathol.* **86**, 215–223.
26. Park, J. H., S. Lee, J. H. Kim, K. Park, K. Kim and I. C. Kwon (2008) Polymeric nanomedicine for cancer therapy. *Prog. Polym. Sci.* **33**, 113–137.
27. Alexis, F., J. W. Rhee, J. P. Richie, A. F. Radovic-Moreno, R. Langer and O. C. Farokhzad (2001) New frontiers in nanotechnology for cancer treatment. *Urol. Oncol.* **26**, 74–85.
28. Torchilin, V. P. (2001) Structure and design of polymeric surfactant-based drug delivery systems. *J. Control Release* **73**, 137–172.
29. Nishiyama, N., Y. Morimoto, W. D. Jang and K. Kataoka (2009) Design and development of dendrimer photosensitizer-incorporated polymeric micelles for enhanced photodynamic therapy. *Adv. Drug Deliv. Rev.* **61**, 327–338.
30. Rijcken, C. J. F., J. W. Hofman, F. van Zeeland, W. E. Hennink and C. F. van Nostrum (2007) Photosensitiser-loaded biodegradable polymeric micelles: Preparation, characterisation and in vitro PDT efficacy. *J. Control Release* **124**, 144–153.
31. Chowdhary, R. K., N. Chansarkar, I. Sharif, N. Hioka and D. Dolphin (2009) Formulation of benzoporphyrin derivatives in pluronics. *Photochem. Photobiol.* **77**, 299–303.
32. Sezgin, Z., N. Yuksel and T. Baykara (2007) Investigation of pluronic and PEG-PE micelles as carriers of meso-tetraphenyl porphine for oral administration. *Int. J. Pharm.* **332**, 161–167.
33. Roby, A., S. Erdogan and V. P. Torchilin (2006) Solubilization of poorly soluble PDT agent, meso-tetraphenylporphin, in plain or immunotargeted PEG-PE micelles results in dramatically improved cancer cell killing in vitro. *Eur. J. Pharm. Biopharm.* **62**, 235–240.
34. Ma, L. L., P. Jie and S. S. Venkatraman (2008) Block copolymer "stealth" nanoparticles for chemotherapy: Interactions with blood cells in vitro. *Adv. Funct. Mat.* **18**, 716–725.
35. Mondon, K., R. Gurny and M. Möller (2008) Colloidal drug delivery systems: recent advances with polymeric micelles. *Chimia* **62**, 832–840.
36. Trimaille, T., R. Gurny and M. Möller (2004) Synthesis and ring-opening polymerization of new monoalkyl-substituted lactides. *J. Polym. Sci. Part A: Polym. Chem.* **42**, 4379–4391.
37. Mondon, K., M. Zeisser-Labouèbe, R. Gurny and M. Möller (2011) Novel cyclosporin A formulations using MPEG-hexyl substituted polylactide micelles: A suitability study. *Eur. J. Pharm. Biopharm.* **77**, 56–65.
38. Zeisser-Labouèbe, M., N. Lange, R. Gurny and F. Delie (2006) Hypericin-loaded nanoparticles for the photodynamic treatment of ovarian cancer. *Int. J. Pharm.* **326**, 174–181.
39. Rose, G. S., L. M. Tocco, G. A. Granger, P. J. DiSaia, C. T. Hamilton, A. D. Santin and J. C. Hiserodt (1996) Development and characterization of a clinically useful animal model of epithelial ovarian cancer in the Fischer 344 rat. *Am. J. Obstet. Gynecol.* **175**, 593–599.
40. Lange, N., J. P. Ballini, G. Wagnieres and H. van den Bergh (2001) A new drug-screening procedure for photosensitizing agents used in photodynamic therapy for CNV. *Invest. Ophthalmol. Vis. Sci.* **42**, 38–46.
41. Vargas, A., B. Pegaz, E. Debefve, Y. Konan-Kouakou, N. Lange, J. P. Ballini, H. van den Bergh, R. Gurny and F. Delie (2004) Improved photodynamic activity of porphyrin loaded into nanoparticles: An in vivo evaluation using chick embryos. *Int. J. Pharm.* **286**, 131–145.
42. Lee, H. B. and M. D. Blaufox (1985) Blood volume in the rat. *J. Nucl. Med.* **26**, 72–76.
43. Torchilin, V. (2010) Tumor delivery of macromolecular drugs based on the EPR effect. *Adv. Drug Deliv. Rev.* (In press, doi:10.1016/j.addr.2010.03.011).
44. Burt, H. M., X. C. Zhang, P. Toleikis, L. Embree and W. L. Hunter (1999) Development of copolymers of poly(D,L-lactide) and methoxypolyethylene glycol as micellar carriers of paclitaxel. *Colloid Surf. B* **16**, 161–171.
45. Owens, D. E. III and N. A. Peppas (2006) Opsonization, biodistribution, and pharmacokinetics of polymeric nanoparticles. *Int. J. Pharm.* **307**, 93–102.
46. Li, S. D. and L. Huang (2010) Stealth nanoparticles: High density but sheddable PEG is a key for tumor targeting. *J. Control Release* **145**, 178–181.
47. Trimaille, T., K. Mondon, R. Gurny and M. Möller (2006) Novel polymeric micelles for hydrophobic drug delivery based on biodegradable poly(hexyl-substituted lactides). *Int. J. Pharm.* **319**, 147–154.
48. Nottelet, B., C. Di Tommaso, K. Mondon, R. Gurny and M. MöÂller (2010) Fully biodegradable polymeric micelles based on hydrophobic- and hydrophilic-functionalized poly(lactide) block copolymers. *J. Polym. Sci. A Polym. Chem.* **48**, 3244–3254.
49. Kohler, M., J. Gafert, J. Friedrich, H. Falk and J. Meyer (1996) Hole-burning spectroscopy of proteins in external fields: Human

serum albumin complexed with the hypericinate ion. *J. Phys. Chem.* **100**, 8567–8572.
50. Crnolatac, I., A. Huygens, P. Agostinis, A. R. Kamuhabwa, A. Van Aerschot and P. A. M. De Witte (2007) In vitro accumulation and permeation of hypericin and lipophilic analogues in 2-D and 3-D cellular systems. *Int. J. Oncol.* **30**, 319–324.
51. Torchilin, V. P. (2002) PEG-based micelles as carriers of contrast agents for different imaging modalities. *Adv. Drug Deliv. Rev.* **54**, 235–252.
52. Nagayasu, A., K. Uchiyama and H. Kiwada (1999) The size of liposomes: A factor which affects their targeting efficiency to tumors and therapeutic activity of liposomal antitumor drugs. *Adv. Drug Deliv. Rev.* **40**, 75–87.
53. Kawaguchi, T., T. Honda, M. Nishihara, T. Yamamoto and M. Yokoyama (2009) Histological study on side effects and tumor targeting of a block copolymer micelle on rats. *J. Control Release* **136**, 240–246.
54. Tannock, I. F. and D. Rotin (1989) Acid pH in tumors and its potential for therapeutic exploitation. *Cancer Res.* **49**, 4373–4384.
55. Engin, K., D. B. Leeper, J. R. Cater, A. J. Thistlethwaite, L. Tupchong and J. D. McFarlane (1995) Extracellular pH distribution in human tumours. *Int. J. Hyperther.* **11**, 211–216.
56. Yamamoto, Y., Y. Nagasaki, Y. Kato, Y. Sugiyama and K. Kataoka (2001) Long-circulating poly(ethylene glycol)-poly (-lactide) block copolymer micelles with modulated surface charge. *J. Control Release* **77**, 27–38.
57. Ishida, T. and H. Kiwada (2008) Accelerated blood clearance (ABC) phenomenon upon repeated injection of PEGylated liposomes. *Int. J. Pharm.* **354**, 56–62.
58. Koide, H., T. Asai, K. Hatanaka, T. Urakami, T. Ishii, E. Kenjo, M. Nishihara, M. Yokoyama, T. Ishida, H. Kiwada and N. Oku (2008) Particle size-dependent triggering of accelerated blood clearance phenomenon. *Int. J. Pharm.* **362**, 197–200.